Supporting Information

Templated Growth of Perovskite Shells on Single Walled Carbon Nanotubes: A Solution Processable Route Towards Tailored Devices

Gririraj Manoharan, Xuan Li, Stoichko Dimitrov* and Matteo Palma*

Department of Chemistry, Queen Mary University of London, London E1 4NS, United Kingdom

*E-mail: s.dimitrov@qmul.ac.uk; m.palma@qmul.ac.uk

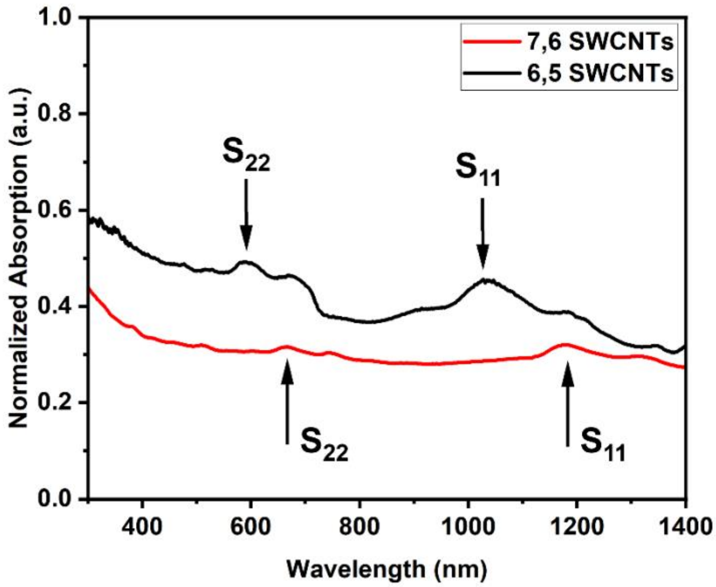

Figure S1. Absorption spectra of pristine (7,6) and (6,5) single walled carbon nanotubes dispersed in DMF. S_{11} and S_{22} transitions of (7,6) and (6,5) chiralities are marked with arrows.

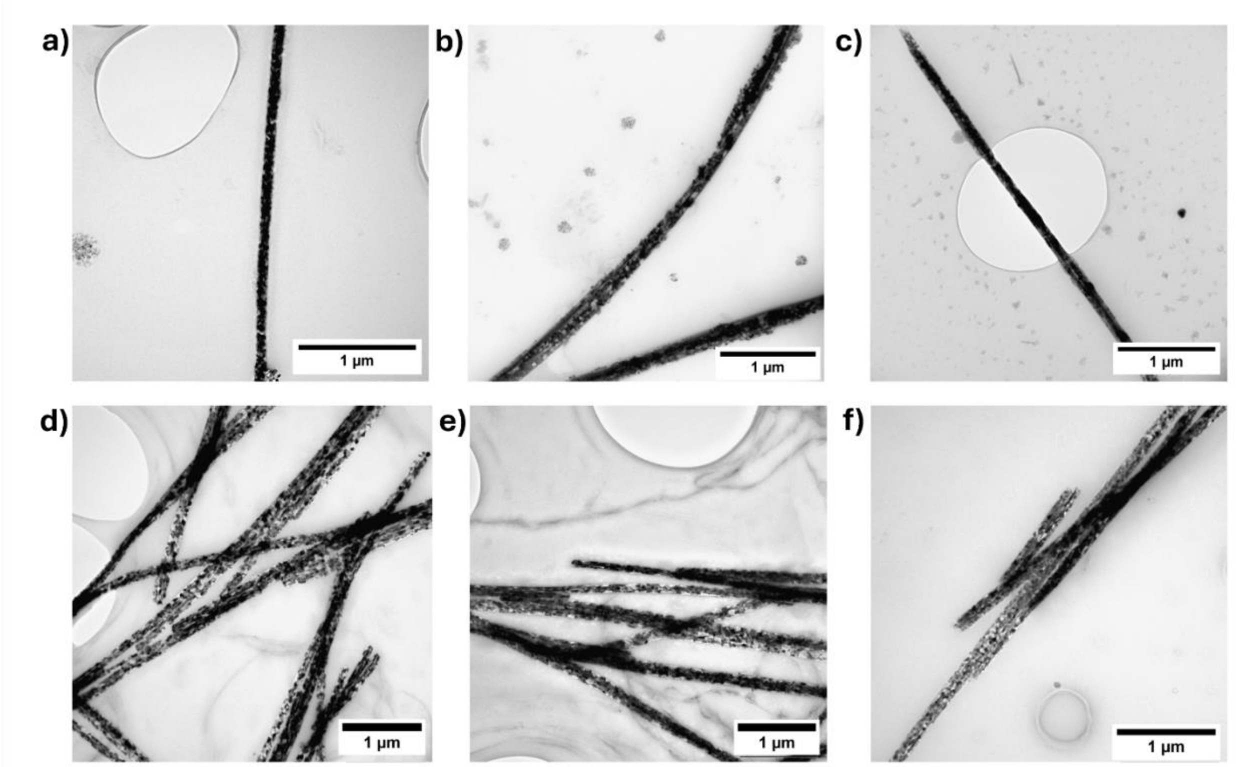

Figure S2. TEM images of SWCNTs-perovskite nanohybrid bundles: a) (7,6) SWCNT-$MAPbI_3$, b) (6,5) SWCNT-$MAPbI_3$, c) (ss) SWCNT-$MAPbI_3$, d) (7,6) SWCNT-$CsPbI_3$, e) (6,5) SWCNT-$CsPbI_3$, and f) (ss) SWCNT-$CsPbI_3$.

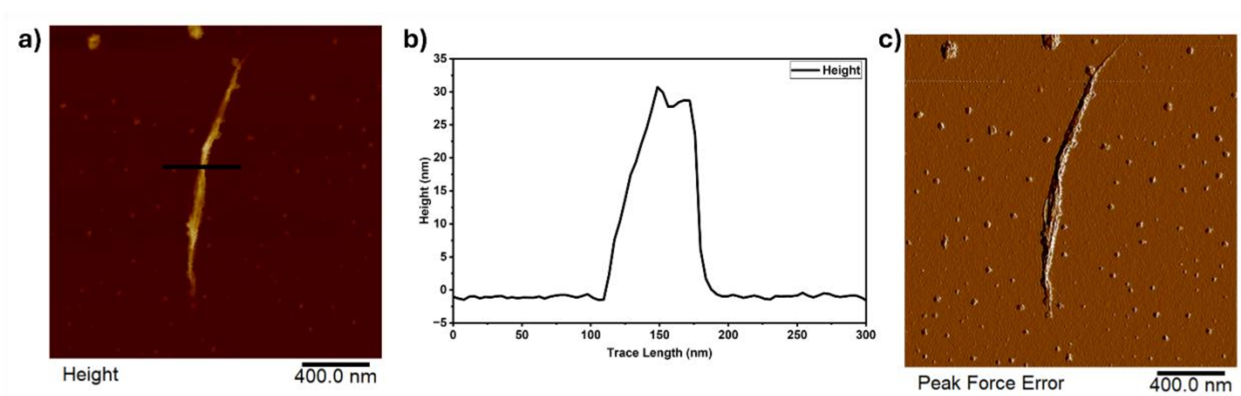

Figure S3. AFM images of a characteristic 7,6 SWCNT-$MAPbI_3$ nanohybrid bundle: a) height image of the nanohybrids, b) height profile of the bundle, and c) peak force error image.

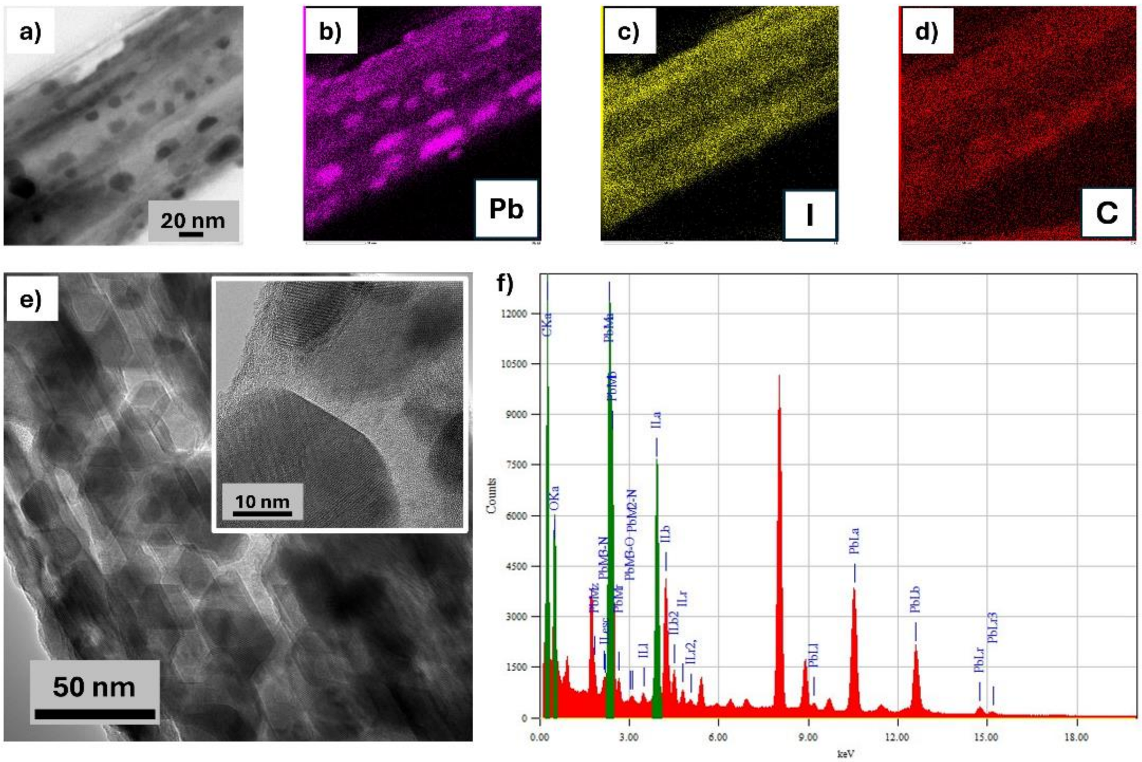

Figure S4. HRTEM image and EDS mapping of the perovskite elements of (7,6) SWCNT-$MAPbI_3$ nanohybrid bundle. a) HRTEM image, b) Pb, c) I and d) C. e) Combined HRTEM image of the nanohybrid bundle and the inset shows the zoomed in image. f) EDS spectra of the same region showing the elements in the nanohybrids. The atomic percentages obtained from the EDS spectrum are C (54.25%), O (16.18%), I (14.33%), and Pb (15.24%). Considering the contribution of the SWCNTs substrate to the carbon signal and possible surface oxidation, it is reasonable to exclude C and O from the stoichiometric analysis; the resulting Pb to I atomic ratio is then 1.06:1. This deviation from the ideal 1:3 ratio of $MAPbI_3$, is likely attributed to iodine loss under electron beam irradiation and the limited quantitative accuracy of EDS in carbon-based hybrid systems.

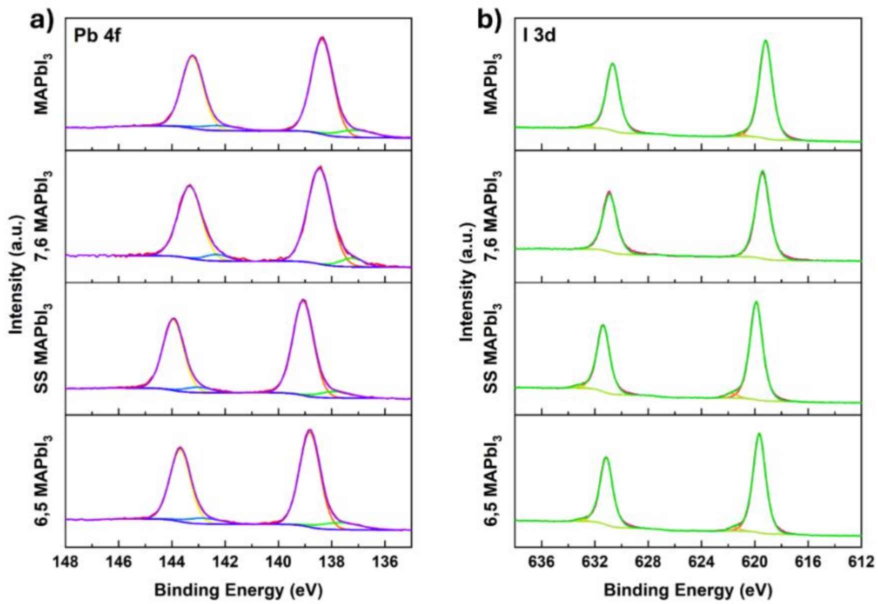

Figure S5. X-ray photoelectron spectroscopy of $MAPbI_3$ perovskite film and SWCNT-$MAPbI_3$ nanohybrids for three chiralities (7,6), (6,5) and ss SWCNTs. a) Pb 4f, b) I 3d.

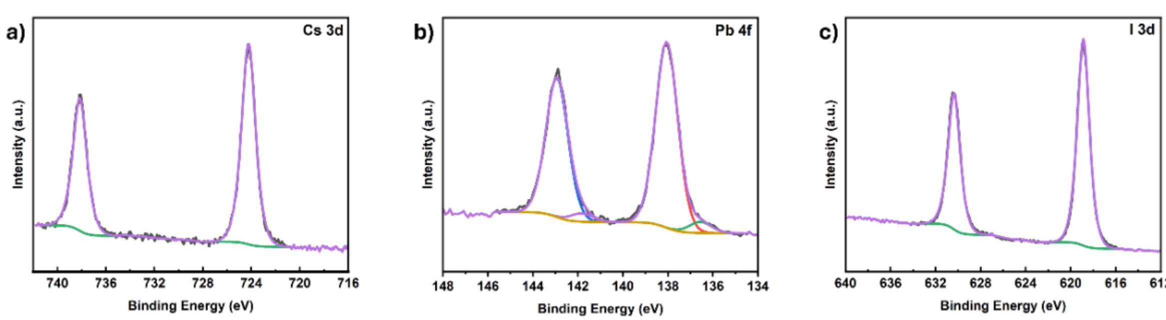

Figure S6. XPS Spectroscopy of 7,6 SWCNT-$CsPbI_3$ nanohybrids confirming the primary elements of the $CsPbI_3$ perovskite a) Cs 3d b) Pb 4f and c) I 3d.

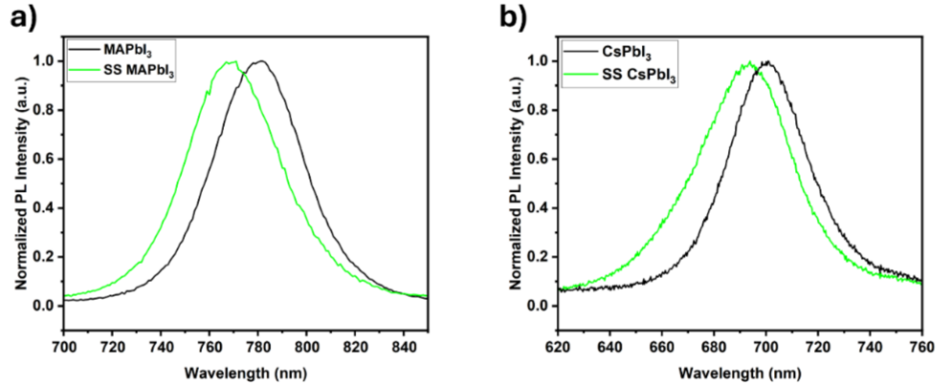

Figure S7. Steady state photoluminescence spectra of perovskite films a) $MAPbI_3$ and b) $CsPbI_3$ and their perovskite nanohybrids with (ss) mixed chirality carbon nanotubes.

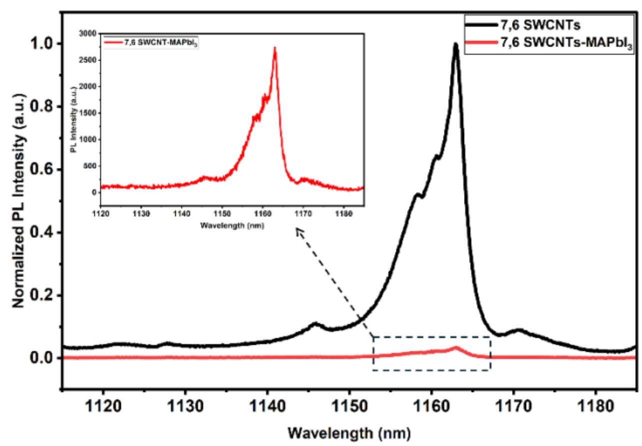

Figure S8. Normalized photoluminescence spectra of 7,6 SWCNTs (Black) and 7,6 SWCNTs-$MAPbI_3$ (Red) at 1150 nm. (Inset: Zoomed in view of PL spectra of SWCNT-$MAPbI_3$ of the same sample). The PL spectra were acquired under 532 nm excitation, monitoring the characteristic emission of the nanotubes (1150 nm) for (7,6 SWCNTs and 7,6 SWCNT-$MAPbI_3$)

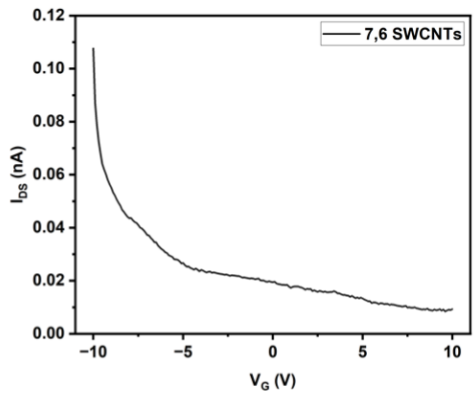

Figure S9. Transfer characteristics of the pristine (7,6) single walled carbon nanotubes FET.

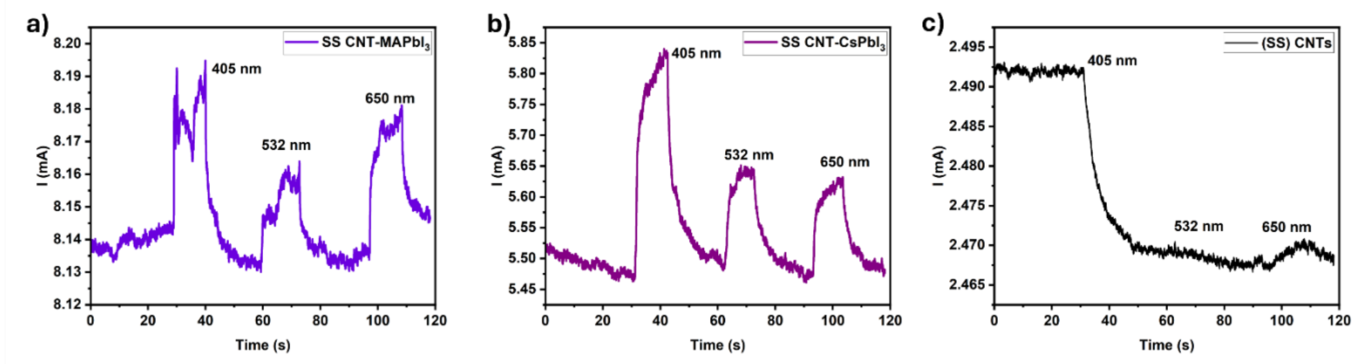

Figure S10. Photoresponse characteristics of the short SWCNTs nanohybrids at different wavelengths (405 nm, 532 nm and 650 nm) for a) ss SWCNT-$MAPbI_3$, b) ss SWCNT-$CsPbI_3$ and c) ss SWCNTs hybrids, in vacuum.

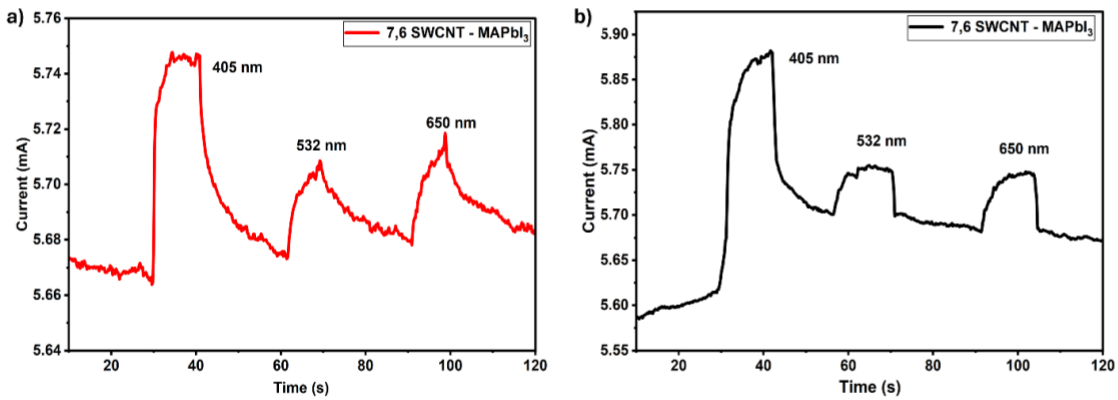

Figure S11. Stability test of the SWCNT-Perovskite photoresponsive device. Photoresponse measurement of a) 7,6 SWCNT-$MAPbI_3$ nanohybrid device , and b) of the same device stored in air for a week.

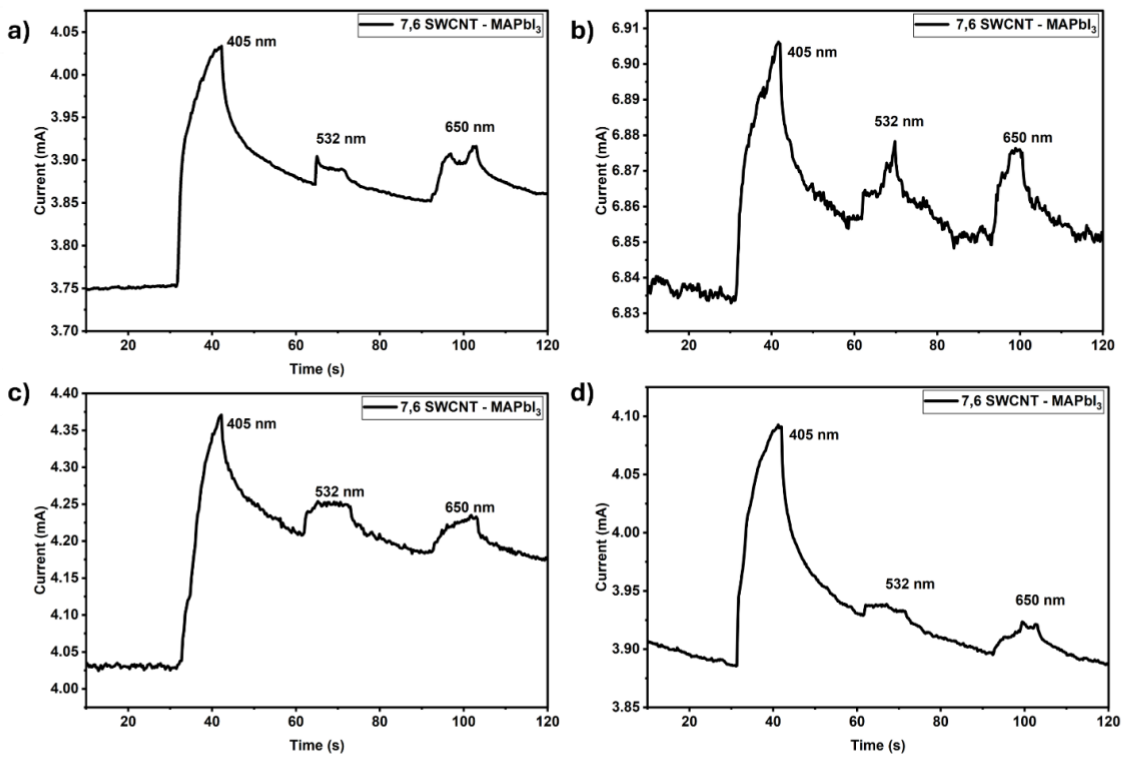

Figure S12. Reproducibility test of the SWCNT-perovskite photoresponsive devices prepared from different perovskite batches. (a-d) 7,6 SWCNT-$MAPbI_3$ photoresponsive devices and their corresponding photoresponse upon different wavelength illuminations.

Table S13. Responsivity of the carbon nanotube-perovskite nanohybrids at three different laser wavelengths illuminations.

Responsivity (A/W)	405 nm	532 nm	650 nm
7,6 $MAPbI_3$	2.71E+03	2.26E+03	8.42E+03
6,5 $MAPbI_3$	5.43E+03	4.41E+03	1.71E+04
7,6 $CsPbI_3$	7.54E+03	6.23E+03	2.30E+04
6,5 $CsPbI_3$	8.14E+03	6.83E+03	2.53E+04
ss $MAPbI_3$	1.59E+03	1.34E+03	4.98E+03
ss $CsPbI_3$	1.13E+03	9.25E+02	3.42E+03

Table S14. Detectivity of the carbon nanotube-perovskite nanohybrids at three different laser wavelengths illuminations.

Detectivity (Jones)	405 nm	532 nm	650 nm
7,6 $MAPbI_3$	1.93539E+12	4.2426E+11	6.02192E+12
6,5 $MAPbI_3$	3.17709E+12	6.7599E+11	9.99342E+12
7,6 $CsPbI_3$	3.58276E+12	7.7546E+11	1.09188E+13
6,5 $CsPbI_3$	3.61518E+12	7.9446E+11	1.12454E+13
ss $MAPbI_3$	6.7053E+11	1.4879E+11	2.10867E+12
ss $CsPbI_3$	4.10642E+11	8.8258E+10	1.24838E+12

Characterizations: SWCNTs-perovskite nanohybrids

Shimadzu UV-3600 Plus instrument was employed to carry out the absorption spectra analysis of the pristine single walled carbon nanotubes with enriched chirality (7,6) and (6,5) in solution. The measurements were performed in a cuvette with optical length of 10 mm.

Panalytical CubiX3 X-ray powder diffractometer was operated under the following conditions for acquiring XRD spectra: θ-2θ scan measurements were carried out in standard reflection mode, Cu-Kα, divergence slit, Ni-filter, 5-70°. Samples were spin coated on ITO substrates and stored in vacuum containers.

Thermo Fisher Scientific Nexsa X-ray Photoelectron Spectrometer was operated to obtain XPS spectra for all the samples with the following parameters: Source Gun Type: Al K-Alpha, Spot Size: 400 µm, Lens Mode: Standard. Samples were prepared on ITO substrates and stored in a vacuum container.

Raman spectra were recorded on a Renishaw invia reflex spectrometer system. The system was calibrated with silicon chips (standard Raman peak is at 521 cm^{-1}). Samples were measured under 442 nm, 633 nm light sources. Glass substrates were used to prepare the samples. A Renishaw system was employed to perform photoluminescence (PL) measurements and the samples were spin coated on silicon substrates. WIRE Software was employed to perform the measurements. The samples (7,6 SWCNTs and 7,6 SWCNTs-$MAPbI_3$) were prepared separately and excited using a 532 nm laser, emission was collected across the surface in a raster-scanning configuration. Laser source 532 nm, Acquisitions: 3 per line, Grating: IR grating. Emission region the samples were measured at 1150 nm for both pristine 7,6 SWCNTs and 7,6 SWCNT-$MAPbI_3$ nanohybrids.

EdinburghFLS1000 steady state spectrometer was utilized for photoluminescence spectroscopy, equipped with a 450 W ozone-free xenon arc lamp with two detector paths: PMT-900 GR for 400 nm and NIR PMT-1400 for near-infrared detection. For time-resolved photoluminescence (TRPL) measurements, EPL-375 picosecond pulsed laser diodes and 635 nm laser sources were employed.

Scanning Electron Microscope (SEM) images were acquired from FEI Inspect-F equipped with EDS. Pristine nanotubes, Si-SiO_2 substrates with interdigitated electrodes (3 μm) (X&X Technology, UK), and SWCNT-perovskite nanohybrids photo responsive FET devices were imaged using this set up.

Atomic force microscopy (Bruker Dimension Icon, Bruker, Karlsruhe, Germany) was carried out to image the SWCNT-$MAPbI_3$ nanohybrid bundles spin coated on a silicon substrate in non-contact mode (Bruker ScanAsyst Air Tips).

Transmission electron microscopy (TEM) images were obtained from JEOL F200 equipped with EDS. Holey carbon film copper grids (Agar Scientific Ltd., UK) were employed to drop cast the carbon nanotube-perovskite-EA mixture and then annealed at 100 °C and then dried in glove box environment overnight.

Transfer characteristics and light responses of bare SWCNT FETs and Perovskite-CNT FETs were conducted on a four probes platform (Lakeshore) equipped with a semiconductor characterization system (Keithley 4200SCS). Gate voltage sweep: -10 V to 10 V. 405 nm, 532 nm and 650 nm illuminations were generated by laser pointer light sources.